Crystal Growth, Magnetic, and Optical Properties of the Ternary Nitride $MnSiN_2$

Saeid Esmaeilzadeh,*,† Ulf Hålenius,‡ and Martin Valldor§

Department of Inorganic Chemistry, Arrhenius Laboratory, Stockholm University, SE-106 91 Stockholm, Sweden, Department of Mineralogy, Swedish Muséum of Natural History, Box 50007, SE-104 05 Stockholm, Sweden, and Institute for Physiscs of Condensed Matter, TU-Braunschweig, Mendelssohnstrasse 3, D-38 106 Braunschweig, Germany

Received February 15, 2006. Revised Manuscript Received March 30, 2006

Single crystals of $MnSiN_2$ have been obtained in dimensions up to several millimeters via a vapor−liquid−solid (VLS) crystal growth mechanism. Detailed single-crystal structure investigations have been carried out. The atomic structure was refined using the space group symmetry $Pna2_1$ and the unit cell parameters $a = 5.2706(12)$, $b = 6.5206(14)$, and $c = 5.0706(12)$ Å. The crystals were transparent with an intense red color, although only spin-forbidden electronic d−d transitions in high-spin Mn^{2+} are expected. Optical absorption spectra show a band structure comparable to spectra of Mn^{2+} in oxide matrixes; however, the absorption bands occur at lower energies and are more intense than expected. This effect is ascribed to a higher degree of covalency for Mn−N bonds. The atomic and magnetic structures have been refined using neutron powder diffraction data collected at room temperature. The magnetic data were collected using a SQUID in the temperature range of 300−700 K in magnetic fields up to 5 T. The paramagnetic region above 500 K contains strong magnetic fluctuations of antiparallel type. Below 490 K, the spins order antiparallel and the magnetic ordering turns into a capped antiferromagnetic state at 442 K with spin tilting disorder.

Introduction

Several new ternary nitridosilicates have been synthesized and structurally investigated in recent years. They have been studied mostly due to their superior mechanical properties, especially at high temperatures. However, up to now, very few nitridosilicates have been investigated for their magnetic or optical properties.

$MnSiN_2$ has previously been synthesized through amonolysis process.[1] The product obtained by amonolysis was presented as a brownish fine powder with anti-ferromagnetic ordering below 180 °C.[2]

Other ternary nitrides have also been reported isostructural to $MnSiN_2$ such as $BeSiN_2$,[3] $MgSiN_2$,[4] $MnGeN_2$,[5] and $ZnGeN_2$.[6] Most of these ternary nitrides have also been synthesized using amonolysis processes.

The magnetic behavior of $MnSiN_2$ is very unusual, possessing an anti-ferromagnetic ordering up to above room temperature. Mn^{2+} containing compounds show usually antiferromagnetic ordering, but the magnetic transition temperatures are much lower.

This paper shows a new synthesis method for $MnSiN_2$, which enables single crystals grown through a VLS mechanism. A detailed structural analysis is presented as well as investigations on optical and magnetic properties.

Experimental Section

$MnSiN_2$ was synthesized using mixtures of Mn and Si_3N_4 powder carefully ground in an agate mortar. Different synthesis conditions, such as synthesis temperature and heating/cooling rates, were tried in order to optimize the crystal growth as well as the product yield. The syntheses were performed in a high-frequency furnace using tungsten crucibles as well as in a tube furnace using alumina boats. No significant differences in the products from the different furnaces could be found. Powder samples of $MnSiN_2$ could be obtained in ≈5.0 g batches by mixing Mn and Si_3N_4 with the Mn:Si ratio of 11:10 (10% excess of Mn). The syntheses were performed in N_2 atmosphere at 1250 °C.

X-ray powder diffractograms collected with a focusing camera of the Guinier-Hägg type, using Cu $K\alpha_1$ radiation and silicon as internal standard, were used for phase identification and unit cell refinement. The films were evaluated with a scanner system.[7]

Supporting Information Available: The single-crystal X-ray diffraction data were collected with an Oxford Diffraction Xcalibur CCD diffractometer with graphite monochromatized Mo Kα radiation ($\lambda = 0.710\,73$ Å) operated at 50 kV and 40 mA. The structure refinement software JANA2000 [8] was used for the single-crystal structure refinement. [The supplementary data have been

* Corresponding author. Telephone: +46-8-161258. Fax: +46-8-152187. E-mail: zaida@inorg.su.se.
† Stockholm University.
‡ Swedish Muséum of Natural History.
§ TU-Branschweig.

(1) Maunaye, M.; Marchand, R.; Guyader, J.; Laurent, Y.; Lang, J. *Bull. Soc. Fr. Mineral. Cristallogr.* **1971**, *94*, 561.
(2) Wintenberger, M.; Marchand, R.; Maunaye, M. *Solid State Commun.* **1977**, *21*, 733.
(3) Eckerlin, P. *Z. Anorg. Allg. Chem.* **1967**, *353*, 225.
(4) David, J.; Laurent, Y.; Lang, J. *Bull. Soc. Fr. Mineral. Cristallogr.* **1970**, *93*, 153.
(5) Wintenberger, M.; Tcheou, F.; David, J.; Lang, J. *Z. Naturforsch., B: Anorg. Chem., Org. Chem.* **1980**, *35*, 604.
(6) Wintenberger, M.; Maunaye, M.; Laurent, Y. *Mater. Res. Bull.* **1973**, *8*, 1049.
(7) Johansson, K. E.; Palm, T.; Werner, P.-E. *J. Phys.* **1980**, *E13*, 1289.

10.1021/cm060382t CCC: $33.50
Published on Web 04/28/2006

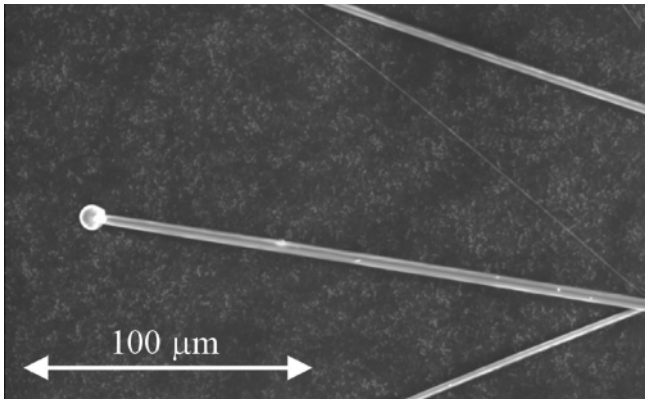

Figure 1. SEM image of $MnSiN_2$ whiskers with the characteristic droplets indicating a VLS crystal growth mechanism.

sent to the Fachinformationzentrum (FIZ) Karlsruhe, Abt. PROKA, 76344 Eggenstein-Leopoldshafen, Germany, as supplementary material No. CSD 416241.]

Neutron powder diffraction (NPD) data were collected at the Studsvik neutron scattering laboratory with $\lambda = 1.47$ Å at room temperature. The Rietveld refinement of the atomic and magnetic structure was performed using the software Fullprof.[9]

The Mn:Si composition and morphology of the $MnSiN_2$ crystals were investigated using a JEOL JSM-820 scanning electron microscope with LINK AN10000 EDX analysis equipment. An Olympus light microscope equipped with a CCD camera was also used for collecting optical images of $MnSiN_2$ single crystals.

Optical absorption spectra were recorded on two selected crystals (thicknesses of 8 and 19 μm, respectively) of high optical quality with a Zeiss MPM 800 microscope−spectrophotometer at ambient (~298 K) and elevated (~510 K) temperatures with a measure spot of 40 μm at a spectral resolution of 1 nm. High-temperature unpolarized spectra were recorded on an absorber placed in a LINKAM TH600 heating stage. The accuracy of the temperature readings was ±10 °C. Due to UV- and IR-opacity of the optics used in the high-temperature experiment, all spectra were measured in a restricted range of the visible spectrum. Each spectrum was analyzed by means of the computer program Jandel PeakFit 4.0, whereby absorption bands were assumed to be of Gaussian shape.

The magnetic data was obtained using a SQUID MPMS-S5 from Quantum Design in the temperature range of 300−700 K in fields of up to 5 T.

Results

The final synthesized products were obtained as reddish powder as well as single crystals with intense red color. The single crystals were often found attached to a solidified droplet of a melt with metallic luster. EDX analysis performed in the scanning electron microscope showed a Mn:Si composition of 1:1 for the red $MnSiN_2$ single crystals, as expected. The metallic droplets were found to possess an Mn:Si ratio of 2:1. The crystals were found in many shapes and sizes; however, some features can be pointed out, such as whiskers, as illustrated in Figure 1. The whiskers of $MnSiN_2$ were formed with squared bases, thicknesses of 1−10 μm, and lengths of up to several millimeters.

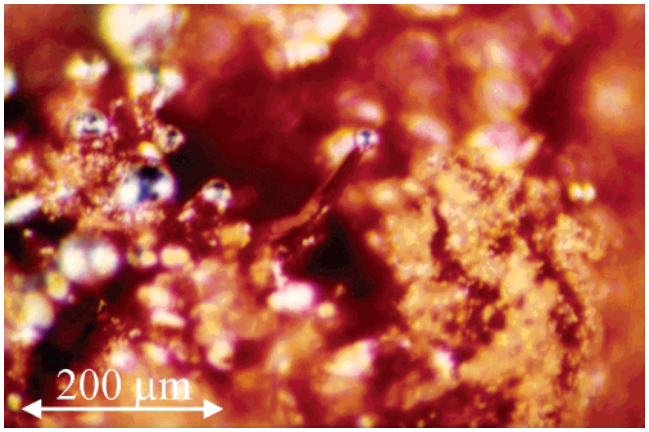

Figure 2. Optical microscope image of intense red $MnSiN_2$ crystals.

Table 1. Data Collection and Crystal Parameters for $MnSiN_2$

chemical formula	$MnSiN_2$
fw (g/mol)	111.1
space group	$Pna2_1$
a (Å)	5.2706(12)
b (Å)	6.5206(14)
c (Å)	5.0706(12)
V(Å^3)	174.26(7)
ρ (g/cm^3)	4.231
crystal size (mm)	0.01 × 0.02 × 0.02
diffractometer	Oxford Diffraction Xcalibur CCD
radiation type	Mo Kα
wavelength (Å)	0.710 73
2θ range (deg)	4.97−34.52
μ (mm^{-1})	7.73
absorption correction	numerical from crystal shape
T_{min}, T_{max}	0.874, 0.964
no. of measrd reflecns	3629
no. of independent reflecns	700
no. of obsd reflecns	550
criterion for obsd reflecns	$I \geq 3\sigma(I)$
R_{int}	0.035
h, k, l, m range	$-8 \leq h \leq 8$ $-10 \leq k \leq 9$ $-7 \leq l \leq 7$
Refinement on R-factors of obsd reflecns	F^2
R, R_w	0.035, 0.090
goodness of fit	1.58
no. of reflecns used in refinement	700
no. of params used in refinement	36
weighting scheme	$1/(\sigma^2(I) + 0.0016I^2)$
residual electron density: max., min. (e/Å^3)	1.4, −3.3

Table 2. Atomic Positions for $MnSiN_2$ Obtained from Single-Crystal XRD Data

	Wyckoff	x	y	z	U_{iso}
Mn	4a	0.077 73(9)	0.624 10(8)	0.00	0.006 14(16)
Si	4a	0.067 91(16)	0.124 99(15)	0.007 0(7)	0.004 5(3)
N1	4a	0.114 6(6)	0.660 6(5)	0.419 8(10)	0.005 7(8)
N2	4a	0.047 0(6)	0.088 9(6)	0.346 2(11)	0.006 0(8)

For larger crystals the droplets were found to be larger and the shape of the crystals were usually more pyramidal or cone-shaped, as illustrated in Figure 2. This indicates that the droplet is consumed during the crystallization process

Structure Refinements. The structural refinement using single-crystal XRD data was performed using the structure model published by Maunaye et al.[1] There are four atomic positions in the unit cell, and a total number of 36 structural parameters were refined, including anisotropic displacement parameters. The crystal structure parameters, the refined atomic positions, and the anisotropic displacement parameters are listed in Tables 1−3, respectively. Additionally, a few

(8) Petricek, V.; Dusek, M. Institute of Physics AVCR, Praha, Czech Republic, 1997.
(9) Roisnel T.; Rodriguez-Carvajal, J. *Fullprof2k V. 1.8a*; Laboratoire Léon Brillouin (CEA-CNRS): Gif-sur-Yvette Cedex, France, 2001.

Table 3. Anisotropic Displacement Parameters for $MnSiN_2$ Obtained from Single-Crystal XRD Data

	U_{11}	U_{22}	U_{33}	U_{12}	U_{13}	U_{23}
Mn	0.0057(2)	0.0068(3)	0.0059(3)	0.00023(16)	0.0001(3)	0.0001(3)
Si	0.0033(4)	0.0062(4)	0.0038(5)	0.0000(3)	−0.0004(6)	0.0000(5)
N1	0.0038(11)	0.0064(16)	0.0070(15)	−0.0003(11)	−0.0001(10)	−0.0008(11)
N2	0.0064(12)	0.0062(16)	0.0054(15)	−0.0014(11)	−0.0003(11)	−0.0005(13)

Table 4. Selected Interatomic Distances and Angles

involved atoms	distance (Å) or angle (deg) (std. dev.)
Mn−N	2.132(4), 2.139, 2.151(5), 2.154(4)
Si−N	1.725(5), 1.739(7), 1.746(3), 1.753(4)
Mn−Mn	2 × 3.1050(7), 2 × 3.1174(4)
Mn−N−Mn	2 × 93.30(13), 2 × 92.81(16)

Table 5. Atomic Positions and Isotropic Displacement Parameters for $MnSiN_2$ Obtained from NPD Data

	Wyckoff	x	y	z	B_{iso}
Mn	4a	0.077(1)	0.624(1)	0.00	0.58(14)
Si	4a	0.067(1)	0.126(1)	0.006(2)	0.29(1)
N1	4a	0.1133(5)	0.6593(5)	0.420(2)	0.524(5)
N2	4a	0.0478(5)	0.0906(6)	0.348(1)	0.509(5)

bond angles and distances from the single-crystal refinement are presented in Table 4.

The NPD data collected at room temperature show both diffraction peaks originating from atomic structure and magnetic ordering. The pattern reveals two strong reflections of purely magnetic origin, namely, the 100 and 101 reflections, of which both break the *a*-glide and the 2_1 symmetries found in the space group $Pna2_1$.

In the Rietveld refinement the space group $P\bar{1}$ was used for the magnetic structure. The atomic structure was refined using the reflections in the range $2\theta = 13-140°$, and the magnetic reflections in the range $2\theta = 13-60°$ were used to model the magnetic structure. A total number of 37 parameters was refined: 11 positional parameters and 4 isotropic thermal displacement parameters. An impurity phase, identified as Si_2N_2O,[10] was included in the refinement. The fit between the observed and the calculated NPD data is shown in Figure 3.

The refined atomic coordinates and the thermal displacement parameters are given in Table 5. Only one parameter was used for the refinement of the magnetic structure, namely, the magnetic moment for the Mn atoms, with a refined value of 3.55(5) μ_B. All spin directions were chosen to be parallel with the *c*-axis, on the basis of the earlier proposed magnetic structure.[2] The residuals for the atomic structure in the neutron data (212 reflections) were $\chi^2 = 3.0$, $R_{wp} = 0.063$, $R_p = 0.055$, Dwd = 0.88, and $R_F = 0.014$; for the magnetic structure (48 orthorhombic reflections) $R_F = 0.049$.

Description of the Atomic and Magnetic Structure. The structure of $MnSiN_2$ is closely related to the hexagonal wurtzite structure. There are several nitrides possessing a crystal structure similar to the hexagonal wurtzite structure such as AlN,[11] GaN,[12] and InN.[13] In $MnSiN_2$ the trivalent ions Al^{3+}, Ga^{3+}, and In^{3+} are replaced 50% by the divalent Mn^{2+} and 50% by the quadrovalent Si^{4+}. The N^{3-} ions are almost hexagonally close-packed, but a small distortion results in orthorhombicity. The Mn^{2+} and Si^{4+} ordering in $MnSiN_2$ leads finally to an orthorhombic superstructure of the hexagonal wurtzite type structure, where $\mathbf{a}_{ort} = 2\mathbf{a}_{hex} + \mathbf{b}_{hex}$, $\mathbf{b}_{ort} = 2\mathbf{b}_{hex}$, and $\mathbf{c}_{ort} = \mathbf{c}_{hex}$ (ort. = orthorhomic, hex. = hexagonal settings). A polyhedral illustration of the crystal structure of $MnSiN_2$ is shown in Figure 4. The antiferromagnetic ordering, as refined from the NPD data, is illustrated in Figure 5, as antiparallel spins aligned along the crystallographic *c*-axis. The atomic ordering of the Mn atoms is related to the diamond structure, and each Mn atom has four closest neighbors, as in a tetrahedron, with antiparallel spins.

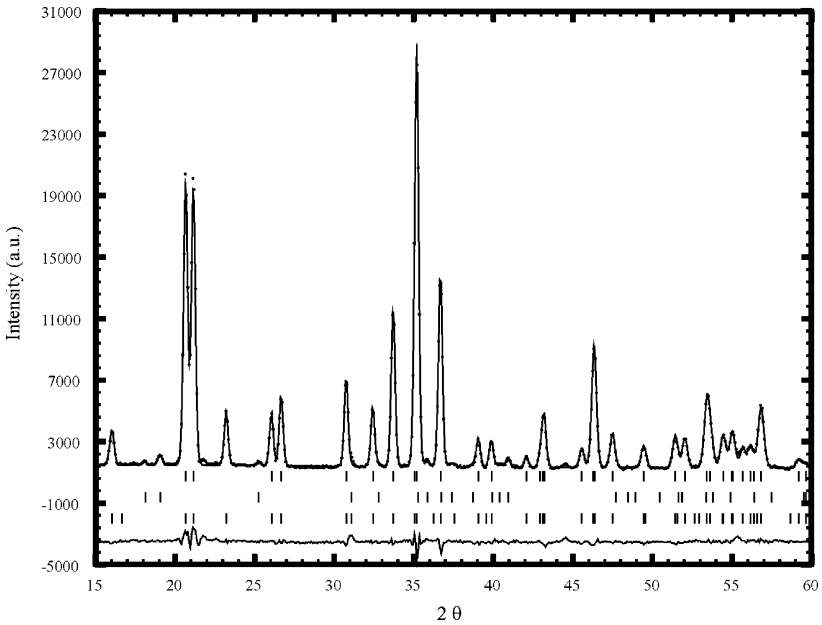

Figure 3. Observed, calculated, and difference NPD pattern of $MnSiN_2$ in the range $2\theta = 15-60°$. The markers, from top to bottom, show the positions of the diffraction peaks of the atomic structure of $MnSiN_2$, the impurity phase of Si_2N_2O, and the magnetic structure of $MnSiN_2$.

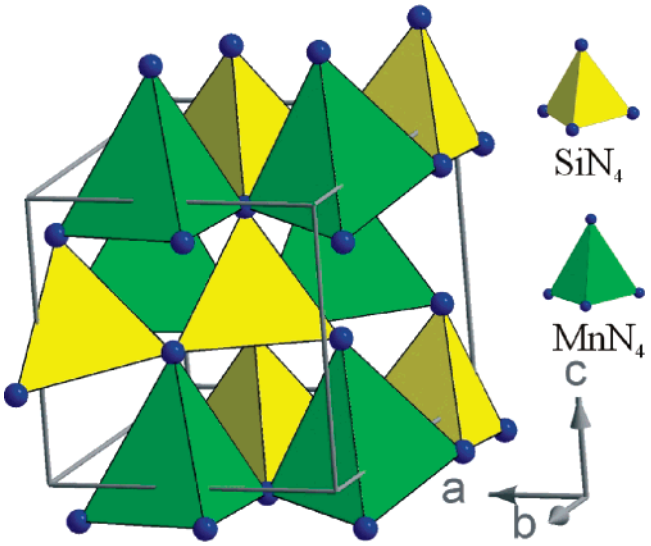

Figure 4. Polyhedral illustration of the $MnSiN_2$ structure.

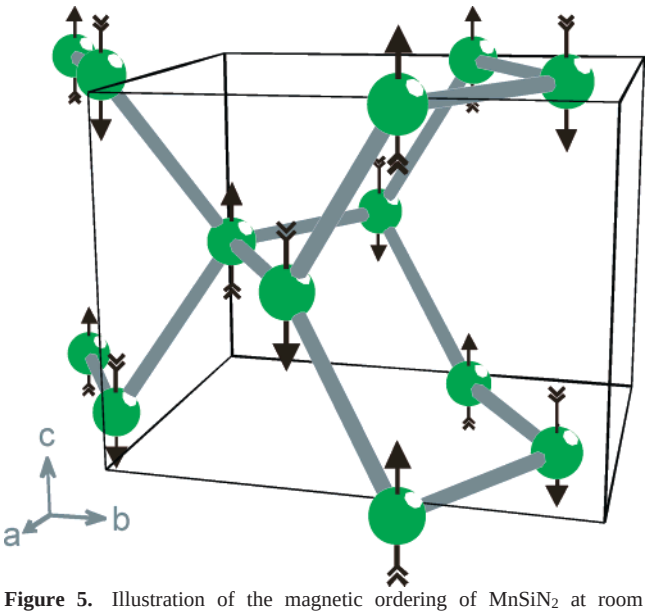

Figure 5. Illustration of the magnetic ordering of $MnSiN_2$ at room temperature. Only the Mn atoms are shown in this illustration.

Magnetic Susceptibility. In the previous report on $MnSiN_2$,[2] an anti-ferromagnetic transition was reported at 180 °C, but nothing further was stated about the magnetic properties. The reinvestigation, presented here, reveals a more complex behavior. Even at the highest measured temperature (700 K), the Mn magnetic moments are not fully decoupled, as full linearity of the $\chi^{-1}(T)$ curve (Figure 6a) is not reached. Despite this, we tried to extract a magnetic moment of Mn and a Weiss constant (θ_{CW}), using the Curie−Weiss formula for the data in the temperature range of 650−700 K. The magnetic moment of Mn (6.87 μ_B) is higher than expected, since 5.9 μ_B is normal for Mn^{2+} (d^5) in a high-spin state,[14] but within experimental errors, since the purely paramagnetic range was not reached.

θ_{CW} is highly negative, which indicates strong antiparallel magnetic fluctuations far above the observed transition temperature. The refined value of $\theta_{CW} = -1984$ K is probably too high, but it is safe to assume that $\theta_{CW} > 1000$ K, which still is very interesting, since $\theta_{CW} \gg T_N$ (500 K). This implies that magnetic frustration must exist in the system. Thermoremnant magnetization at lower temperatures (Figure 6) is further evidence for frustration; a relatively weak outer field (1 T) can tilt spins from their ideal antiparallel formation during the magnetic ordering process.

The broadness of the transition close to 500 K signals that the solidification of the magnetic structure, with antiparallel spins, has a low-dimensional character. At 442 K, the spins turn canted due to frustration.

To account for the relatively low magnetic moment per Mn, from the neutron diffraction data, maybe the spins should be described as canted from the *c*-axis in a disordered fashion. The presence of a field turns this disorder into a more ideal canted anti-ferromagnetic state, similar to a ferrimagnetic state; the dc magnetic field works to cancel out the spin entropy.

The magnetization above and below the critical temperature is linear with the field and displays no hysteresis (Figure 7). The magnetic moment is lower in the fully frozen state than in the high-temperature state, meaning that the magnetic solid has antiparallel spins. No metamagnetic transition is seen up to 5 T. This demonstrates that the low-temperature spin configuration is stable, once it is formed, either with random tilting of the spins or with a long-ranged canting ordering of the spins. The last conclusion is also based on the fact that there is no relaxation of the thermoremnant magnetization (data not shown here).

Optical Spectroscopy. The polarized room-temperature optical absorption spectra display a series of relatively narrow absorption bands (Figure 8) at 18 070, 19 250, 20 040, 21 030, 22 050, 23 810, 24 390, 25 890, and 27 980 cm^{-1}, which compares well with spectra of divalent manganese ($3d^5$) in a large number of salts.[15−17]

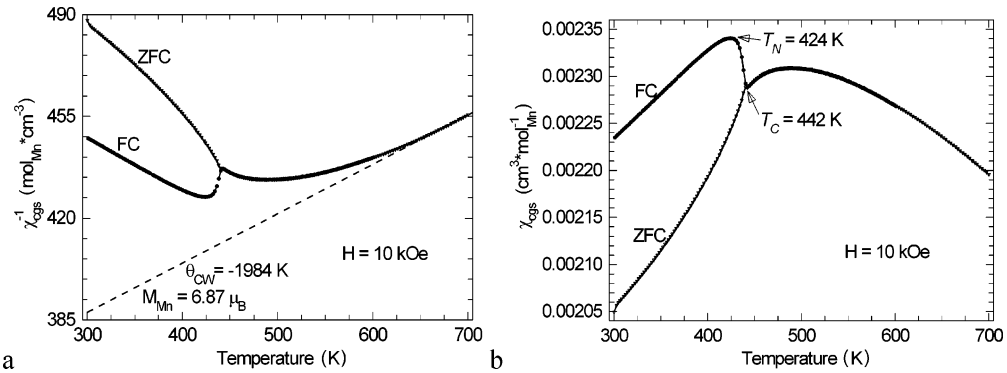

Figure 6. Magnetic susceptibility plotted as functions of temperature. The dashed line in panel a represents the Curie−Weiss behavior extended for the range of 650−700 K.

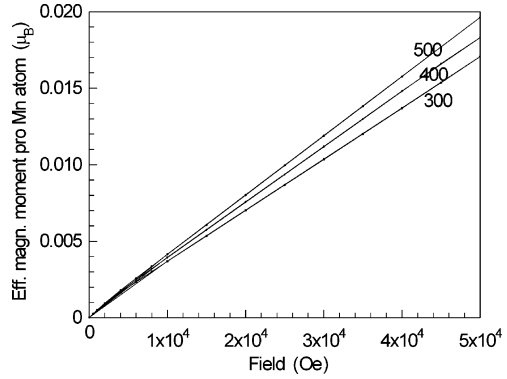

Figure 7. Effective magnetic moment plotted vs applied field. The curves are marked with the temperatures (in kelvin), at which the data were obtained. All three curves contain both an increase and decrease in outer field.

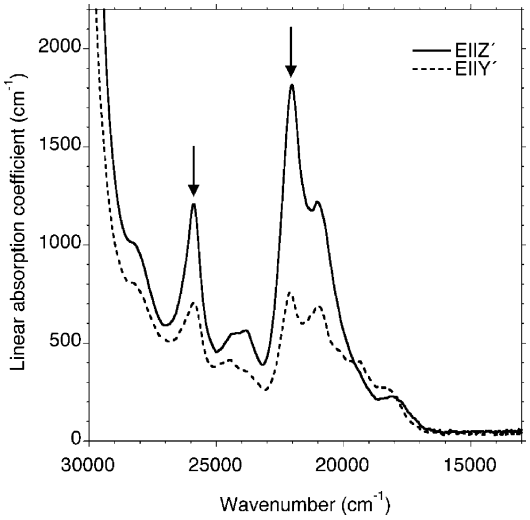

Figure 8. Polarized optical absorption spectra (E||Z′ and E||Y′) of $MnSiN_2$ recorded on an 8 μm thick crystal cut perpendicular to the optical *X*-direction. Arrows mark the bands caused by the field-independent d−d transitions $^6A_{1g}$ (^6S) → $^4E(^4D)$ and $^6A_{1g}$ (^6S) → $^4E^4A_1$ (^4G) in Mn^{2+}.

The absorption bands are assigned to electronic transitions between energy levels from the Mn^{2+} ground state $^6A_{1g}$ (^6S) and excited states derived from ^4G, ^4D, and ^4P. The sharp and intense absorption bands at 22 000 and 25 890 cm^{-1} represent most likely transitions to the field-independent levels $^4E^4A_1$ (^4G) and $^4E(^4D)$, respectively. Based on this tentative assignment, Racah parameters *B* and *C* and the crystal field parameter Dq are calculated to be ca. 550, 3310, and 650 cm^{-1}, respectively. A tetrahedral coordination of Mn^{2+} in $MnSiN_2$ and a higher degree of covalency for Mn^{2+}−N bonds as compared to Mn^{2+}−O bonds explain a shift of absorption bands toward lower energies and comparable low values calculated for *B* and Dq.

The molar absorption coefficients, ϵ, of the observed absorption bands in the present spectra are unusually high,

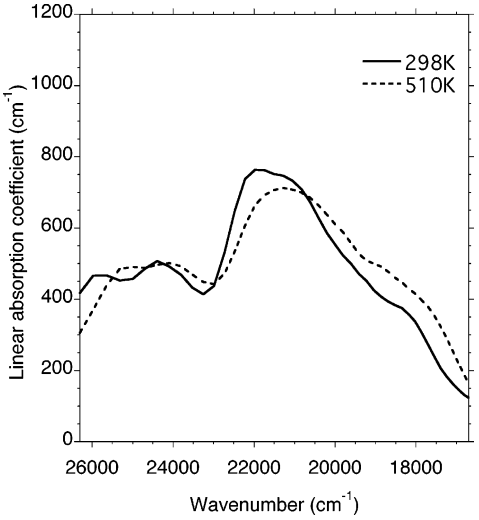

Figure 9. Unpolarized optical absorption spectra of a 19 μm thick unoriented $MnSiN_2$ crystal recorded through the LINKAM TH600 heating stage at 298 and 510 K.

displaying values up to ca. 50 L·mol^{-1}·cm^{-1}, which is about 2 orders of magnitude higher than for bands caused by spin-forbidden transitions in octahedrally coordinated Mn^{2+} in oxygen-based structures and also higher than recorded for bands caused by spin-forbidden transitions in tetrahedrally coordinated $3d^5$ cations in oxygen-based structures.[18]

Unpolarized high-temperature (510 K) spectra of $MnSiN_2$ reveal a band distribution and band intensities comparable to the RT spectra (Figure 9). The main difference is a general shift of ca -400 ± 150 cm^{-1} of absorption bands with increasing temperature and a moderate band broadening. No obvious effects related to a magnetic phase transition are evident in the recorded high-temperature spectrum of $MnSiN_2$.

Discussion

Single crystals of $MnSiN_2$ have been grown through a VLS mechanism involving the melting of Mn metal, dissolving Si_3N_4 powder and N_2 gas. After reaching a certain concentration of the species, the melt is saturated and crystals of $MnSiN_2$ are grown out from the molten solution. The size of the crystals is found to be determined to a large extent by the size of the droplet. The metallic droplet is consumed during the crystallization and, by shrinkage of the droplet, the base of the crystal is decreased and therefore pyramidal-shaped crystals could be formed in many cases.

The strong magnetic interactions are due to superexchange, since all Mn ions are +2, the Mn−N−Mn bond angles are close to 90°, and the Mn−Mn distances are more than 3 Å; the latter observation prevents the occurrence of direct exchange and the fact that all Mn are equivalent eliminates possible double-exchange through electron transfer. The observed magnetic frustration could originate from the fact that there are two almost equal Mn−N−Mn angles (93.3(1) and 92.8(2)°), giving a slight degeneration of the magnetic state. This degeneration might induce a canting of the spins

(10) Sjoeberg, J.; Helgesson, G.; Idrestedt, I. *Acta Crystallogr., Sect. C: Cryst. Struct. Commun.* **1991**, *47*, 2438.
(11) Jeffrey, G. A.; Parry, G. S.; Mozzi, R. L. *J. Chem. Phys.* **1956**, *25*, 1024.
(12) Schulz, H.; Thiemann, K. H. *Solid State Commun.* **1977**, *23*, 815.
(13) Xu, Y.-N.; Ching, W. Y. *Phys. Rev. B* **1993**, *48*, 4335.
(14) West, A. R. *Basic Solid State Chemistry*; John Wiley & Sons: London, England, 1999.
(15) Lohr, L. L.; McClure, D. S. *J. Chem. Phys.* **1968**, *49*, 3516.
(16) McPherson, G. L.; Aldrich, H. S.; Chang, J. R. *J. Chem. Phys.* **1974**, *60*, 534.
(17) Ono, H.; Fuchikama, N. *J. Phys. Soc. Jpn.* **1977** *42*, 1569.
(18) Waychunas, G. A.; Rossman, G. R. *Phys. Chem. Miner.* **1983**, *9*, 212.

of about 1°. This, in turn, would give the system a small degree of freedom, which is dominated by entropy, giving disorder, unless an outer field is applied, resulting in an ordered canted anti-ferromagnetic state. The high molar absorption coefficients recorded for bands caused by spin-forbidden d−d transitions in Mn^{2+} in $MnSiN_2$ are explained by selection rule relaxations caused by the non-centrosymmetric MnN_4 site symmetry in combination with a higher degree of bond covalency and thus a larger potential for ligand and central ion orbital mixing for Mn^{2+}−N as compared to Mn^{2+}−O.

Acknowledgment. Dr. Jekabs Grins is acknowledged for valuable discussions regarding the magnetic structure refinement. S.E. possesses a research fellowship from the Royal Swedish Academy of Sciences financed by the Knut and Alice Wallenberg Foundation. The Swedish Research Council and the Carl Trygger Foundation is acknowledged for financial support.

CM060382T